High-Power Single-Frequency Lasers Using Thin Metal Film Mode-Selection Filters

By PETER W. SMITH, M. V. SCHNEIDER, and HANS G. DANIELMEYER

(Manuscript received December 12, 1968)

In this paper we present the theory of mode selection by use of a thin metal film in the laser cavity and we derive formulae both by a rigorous method and by using a lumped-circuit approach. Experiments performed with a 500-mW argon ion laser showed that 350 mW or 70 percent of the multimode power could be obtained in single-frequency operation using this technique. Somewhat lower efficiencies were obtained with a neodymium-doped yttrium aluminum garnet laser. We compare this with other mode-selection techniques.

I. INTRODUCTION

Troitskii and Goldina recently showed that a thin metal film can be used inside a He-Ne laser cavity to produce single-frequency output.[1] A thin lossy film will favor oscillation on a mode which has a standing-wave minimum at the film position.

The simplicity of this technique is very attractive. We have, therefore, investigated both theoretically and experimentally its efficiency and its application to high power continuous wave (CW) lasers.

In Section II we develop formulas, both rigorously and using a lumped-circuit approach, which relate the complex refractive index of the metal film to its characteristics as a mode filter. We also show how the complex refractive index of a given metal film can be determined from measurements of the reflectivity and transmissivity of the film. Section III describes experiments using this thin-film technique to obtain single-frequency operation of a continuous wave argon ion laser; Section IV describes the results obtained with a neodymium-doped yttrium aluminum garnet laser. In Section V we discuss these results and the applications of this technique.

II. THIN METAL FILMS FOR MODE-SELECTION FILTERS

2.1 *Optical Properties of Thin Metal Films*

The optical properties of a thin metal film can be characterized by a complex index of refraction and by an effective optical thickness. The parameters which are easily measured are transmittance, reflectance, and average physical film thickness. From these parameters one can deduce the index of refraction and the optical thickness. This procedure does not necessarily lead to meaningful optical constants since thin films often consist of separate islands or of material which is considerably different from the bulk metal because of special problems in the deposition process.

Thin metal films can have high losses if the free space transmittance and reflectance are about equal. This property can be used in optical mode selection filters. The film is placed in the null of the E-field of one particular desired mode which experiences little loss because of the film. Undesired modes with nulls in a different plane are attenuated and hopefully eliminated. Best results are obtained for the thinnest film with the highest complex index of refraction. We require that the film be continuous, that is, that is does not consist of a large number of separate aggregates. (But see Ref. 2.) Chromium and titanium are particularly useful materials because they do not tend to form islands on quartz substrates. Continuous thin films can also be obtained with evaporated nickel-chromium alloys (Nichrome) since the high vapor pressure of chromium leads to fractional distillation during evaporation and consequently gives a base layer of chromium directly on the substrate. A further advantage of Nichrome is its high stability with respect to atmospheric contaminants; Nichrome can also be fully evaporated from a tungsten coil.

2.2 *Computation of Reflectance and Transmittance of Thin Metal Films*

The notation used in the following computation is shown in Fig. 1a. The complex index of refraction of the metal film is $N_1 = N - jK$, and the propagation constant in the film, ρ, is given by

$$\rho = \frac{2\pi N_1}{\lambda} \tag{1}$$

where λ is the wavelength in vacuum.

The amplitude reflection and transmission coefficients r and δ for a film with thickness D are[3]

$$r = \frac{(N_2-N_1)(N_1+N_0)\exp(j\rho D)+(N_2+N_1)(N_1-N_0)\exp(-j\rho D)}{(N_2+N_1)(N_1+N_0)\exp(j\rho D)+(N_2-N_1)(N_1-N_0)\exp(-j\rho D)} \quad (2)$$

$$\delta = \frac{4N_2N_1}{(N_2+N_1)(N_1+N_0)\exp(j\rho D)+(N_2-N_1)(N_1-N_0)\exp(-j\rho D)}. \quad (3)$$

Power reflectance R, transmittance T, and loss A are given by

$$R = r r^* \quad (4)$$

$$T = \frac{N_0}{N_2}\delta\delta^* \quad (5)$$

$$A = 1 - R - T. \quad (6)$$

For thin films with $D \ll \lambda$ one can simplify equations (1) and (2) with $\exp(\pm j\rho D) = 1 \pm j\rho D$. In addition we let $N_2 = N_0 = 1$ and obtain

$$r = + \frac{j\rho D(1 - N_1^2)}{2N_1 + j\rho D(1 + N_1^2)} \quad (7)$$

$$\delta = + \frac{2N_1}{2N_1 + j\rho D(1 + N_1^2)}. \quad (8)$$

For $| N_1^2 | \gg 1$ one obtains finally

$$r = - \frac{1}{1 + \frac{2}{j\rho DN_1}} \quad (9)$$

$$\delta = + \frac{1}{1 + \frac{j\rho DN_1}{2}}. \quad (10)$$

This means that the thin film with $| N_1^2 | \gg 1$ can be characterized by one single physical parameter

$$j\rho DN_1 = j\frac{2\pi D}{\lambda}N_1^2. \quad (11)$$

These approximations are appropriate when considering infrared wavelengths. For other cases one has to use the rigorous expressions of equations (2) and (3).

It is often useful to derive an equivalent lumped-film admittance Y based on equations (2) and (3) or equations (7) and (8). The lumped-film admittance Y is shown in Fig. 1b in a transmission line with

admittance Y_2 and Y_0. The reflection and transmission coefficients are

$$r = \frac{Y_2 - Y - Y_0}{Y_2 + Y + Y_0} \tag{12}$$

$$\delta = \frac{2Y_2}{Y_2 + Y + Y_0}. \tag{13}$$

For $Y_2 = Y_0 = 1$ one obtains

$$r = -\frac{1}{1 + \frac{2}{Y}} \tag{14}$$

$$\delta = +\frac{1}{1 + \frac{Y}{2}}. \tag{15}$$

An expression for Y can be obtained from equations (2) or (3). A good approximation valid for thin absorbing films can be derived by using equation (7)

$$r = +\frac{j\rho D(1 - N_1^2)}{2N_1 + j\rho D(1 + N_1^2)} = -\frac{1}{1 + \frac{2}{Y}}. \tag{16}$$

The result for Y is

$$Y = \frac{j\rho D(N_1^2 - 1)}{N_1 + j\rho D}. \tag{17}$$

The rigorous as well as lumped approach have been used for computing transmittance, reflectance, and loss of the film as listed in Table I. The film was one used in the experiments reported in Sections III and IV. The transmittance and reflectance were measured with a traveling-wave beam external to the laser cavity. By successive trials, the value of N_1 was found which gave the best fit to the experimental measurements. One can conclude that this film is thin and lossy enough for using the lumped model.

2.3 *Thin Metal Film in Front of a Mirror*

A thin film in front of a mirror is shown in Fig. 1c. The high reflectance mirror can be considered as a short or open circuit which is spaced by a length L from the back end of the thin metal film. The reflectance and loss can be computed from a rigorous expression derived from equations (2) and (3) or from the approximate model

TABLE I—MEASURED AND COMPUTED THIN FILM PROPERTIES

Film material: Nichrome (80% nickel, 20% chromium)
Film thickness: 50 Å
Wavelength: 10645 Å

	Transmittance T	Reflectance R	Loss A
$N_2 = 1.5$ quartz; $N_0 = 1.0$ air			
Measured	0.78	0.01	0.21
Computed, eqs. (2) and (3), $N - jK = 1.66 - j\cdot 2.83$	0.773	0.0116	0.214
Computed, eqs. (2) and (3) $\exp(\pm j\rho D) = 1 \pm j\rho D$	0.776	0.0115	0.212
Computed, lumped admittance, eq. (17), $Y = 0.272 - j\cdot 0.193$	0.777	0.0115	0.211
$N_2 = 1.0$ air; $N_0 = 1.5$ quartz			
Measured	0.78	0.08	0.14
Computed, eqs. (2) and (3), $N - jK = 1.66 - j\cdot 2.83$	0.773	0.0832	0.143
Computed, eqs. (2) and (3) $\exp(\pm j\rho D) = 1 \pm j\rho D$	0.776	0.0833	0.140
Computed, lumped admittance, eq. (17), $Y = 0.272 - j\cdot 0.193$	0.777	0.0819	0.140

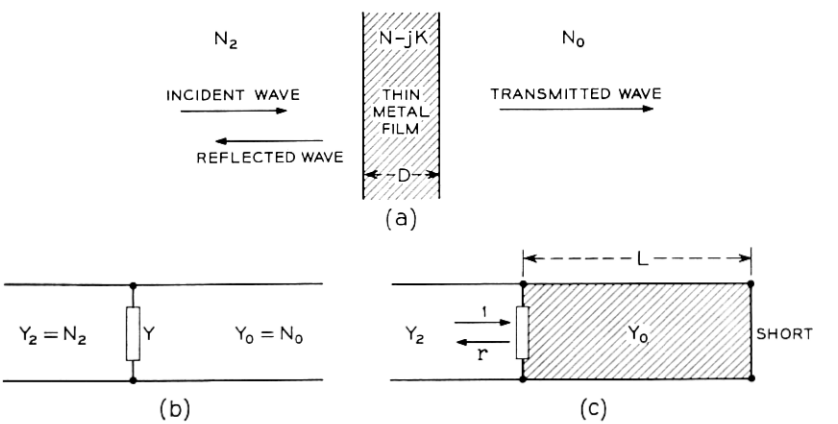

Fig. 1 — Notation used for computing optical film properties: (a) thin metal film with index $N_1 = N - jK$ and thickness D; (b) lumped admittance, $Y = j\rho D(N_1^2 - 1)/(N_1 + j\rho D)$, and (c) admittance Y in front of mirror.

with a lumped admittance Y. The rigorous result for r is

$$r = \frac{E + F}{G + H} \tag{18}$$

where

$$E = (N_2 - N_1)[(N_1N_0 + N_0^2)e^{j\beta} + (N_1N_0 - N_0^2)e^{-j\beta}]e^{j\rho D} \tag{19}$$

$$F = (N_2 + N_1)[(N_1N_0 - N_0^2)e^{j\beta} + (N_1N_0 + N_0^2)e^{-j\beta}]e^{-j\rho D} \tag{20}$$

$$G = (N_2 + N_1)[(N_1N_0 + N_0^2)e^{j\beta} + (N_1N_0 - N_0^2)e^{-j\beta}]e^{j\rho D} \tag{21}$$

$$H = (N_2 - N_1)[(N_1N_0 - N_0^2)e^{j\beta} + (N_1N_0 + N_0^2)e^{-j\beta}]e^{-j\rho D} \tag{22}$$

and

$$\beta = \frac{2\pi N_0 L}{\lambda}. \tag{23}$$

Reflectance obtained from equations (18) to (23) for a 50-Å Nichrome film at $\lambda = 10645$ Å, and a 150-Å film at $\lambda = 5145$ Å is plotted in Fig. 2. The reflectance is plotted as a function of $\Delta\beta/2\pi$ where $\beta = \pi/2 + 2\pi n + \Delta\beta$ and n is an integer. As β can be varied either by changing the film-to-mirror spacing or by changing the frequency of incident radiation, we have written $\Delta\beta = N_0\Delta L/\lambda$ or $N_0L\Delta\nu/c$. The values of N_0 and N_2 are chosen to correspond to the experimental situations in which the films are used. Of particular importance are the minimum and the maximum absorption listed in Table II. Note that if the film has no loss and $N_0 = N_1 = N_2$, the reflectivity is 1 regardless of the value of L or λ.

The data are based on the assumption that the quartz substrate is lossless and that the surface roughness of the substrate is much less than the listed film thickness.

Reflectance and loss can also be computed from the thin-film equivalent circuit of Fig. 1c. The metal film is characterized by the lumped admittance Y, the mirror by a short, and the distance between mirror and film by the effective optical length N_0L. The short is transformed into a susceptance Y_S in parallel with Y given by

$$\frac{Y_S}{Y_0} = -j \cot \frac{2\pi N_0 L}{\lambda}. \tag{24}$$

The reflection coefficient r is

$$r = \frac{Y_2 - Y - Y_S}{Y_2 + Y + Y_S}. \tag{25}$$

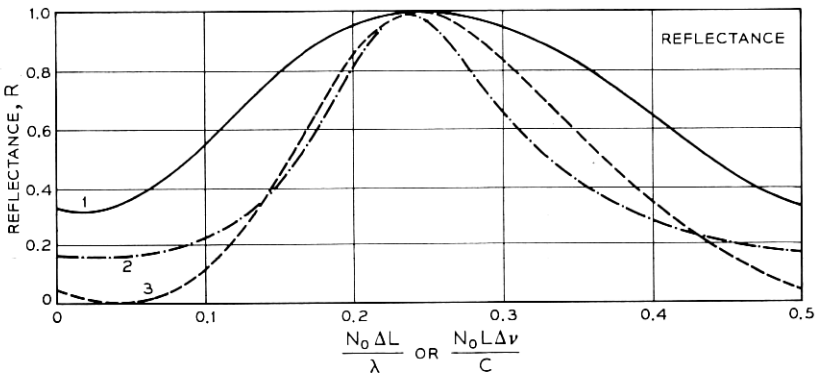

Fig. 2 — Reflectance for mode selectors using 50-Å or 150-Å Nichrome films on quartz substrates as a function of their spacing from the high reflectivity mirror. Notice that the values of N_0, N_2, and λ are chosen to correspond to the experimental circumstances under which each film was used.

Curve	Ni − Cr (Å)	λ (Å)	N_1	N_0	N_2
1	50	10645	$1.66 - j\cdot 2.83$	1.5	1.0
2	150	5145	$1.33 - j\cdot 1.30$	1.0	1.5
3	100	10645	$2.4 - j\cdot 3.5$	1.5	1.0

For the special case $Y_2 = 1$ (air) and $Y_0 = 1.5$ (quartz) one obtains

$$r = \frac{1 - Y + 1.5j \cot (\pi L/\lambda)}{1 + Y - 1.5j \cot (\pi L/\lambda)}. \tag{26}$$

The lumped admittance model always gives a minimum loss of zero because it is based on a limit process in which the film thickness approaches zero while the product $Y \approx j\rho D N_1$ remains constant.

It is clear from the form of equation (25) that the maximum reflectivity comes for $2\pi N_0 L/\lambda = n\pi$ where n is an integer. The fre-

TABLE II—MINIMUM AND MAXIMUM LOSS FOR NICHROME FILMS ON QUARTZ

Film Thickness	Wavelength	Index of refraction $N_1 = N - jk$	N_0	N_2	Minimum loss	Maximum loss
50 Å	10645 Å	$1.66 - j\cdot 2.83$	1.5	1.0	8.5×10^{-5}	0.680
150 Å	5145 Å	$1.33 - j\cdot 1.30$	1.0	1.5	1.3×10^{-2}	0.841

quency spacing between reflectance peaks is just $c/(2N_0L)$. Thus for single-frequency operation the film should be situated sufficiently close to the laser cavity end mirror that $c/(2N_0L)$ is greater than the oscillation width of the laser medium. It is advantageous to make N_0L as large as possible without exceeding this requirement, however, since the selectivity of the mode filter decreases as N_0L is decreased.

The minimum reflectance and the shape of the filter curve in the vicinity of the maximum reflectance are important parameters governing the mode selection properties of the filter. We separate the admittance Y into a real and imaginary part

$$Y = G + jB \tag{27}$$

and obtain from equations (4) and (26) for the reflectance R

$$R = 1 - \frac{4G}{(G+1)^2 + \left(B - 1.5 \cot \frac{\pi L}{\lambda}\right)^2}. \tag{28}$$

The minimum reflectance occurs in the vicinity of the nulls of the cotangent function. Close to maximum reflectance, $\cot(\pi L/\lambda) \gg 1$ and we obtain from equation (28)

$$R = 1 - 1.78G \tan^2 \frac{\pi L}{\lambda}. \tag{29}$$

For rigorous computations one has to use equations (18) to (23). Filter curves based on rigorous equations with $N_1 = N - jK$ as a parameter are shown in Fig. 3. The film thickness for all curves is $D = 150$ Å and the wavelength $\lambda = 5145$ Å.

Notice that we have assumed plane waves in all of these calculations. In practice, if the flat metal film is situated close to a plane laser end mirror, this condition will be well satisfied. If a plane metal film must be situated some distance from the laser end mirrors, the laser cavity must be designed so that there will be a beam waist at the metal film.

The problems encountered in practical filter design are often that films with suitable index of refraction are not stable or *vice versa*. Additional protective coatings have to be deposited which may change the filter characteristics, or a compromise has to be found with one single stable film or two stable films spaced at an appropriate distance inside the laser cavity.

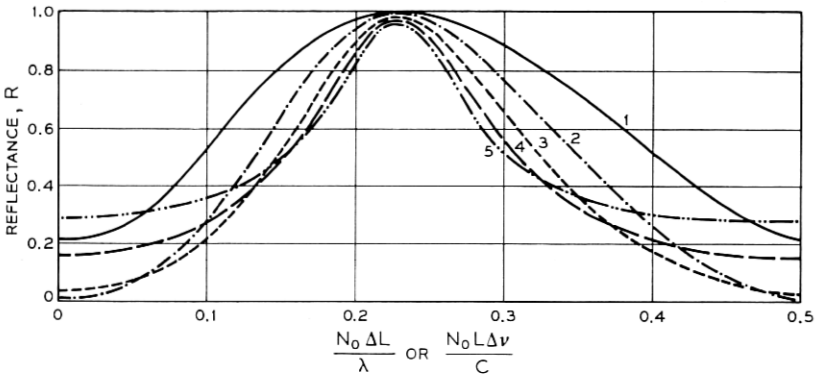

Fig. 3 — Reflectance of a mode selector using a 150-Å metal film for various values of $N_1 = N - jK$: (1) $1 - j$, (2) $1.5 - j \cdot 1.5$, (3) $2 - j \cdot 2$, (4) $2.5 - j \cdot 2.5$, and (5) $3 - j \cdot 3$. The curves are plotted for $\lambda_0 = 5145$ Å, $N_0 = 1.5$, and $N_2 = 1.0$.

2.4 *Film Fabrication*

Films for use as mode selection filters are evaporated from a tungsten coil in a vacuum of $4 \cdot 10^{-7}$ torr. The coils are made from 4-strand tungsten wire with a diameter of 0.015-inch per strand. The source to substrate distance for a 150-Å film is 3.0 inches and the Nichrome charge is a 0.010-inch diameter wire with a length of 0.854 inch. Total evaporation time is less than 10 seconds. The substrates are cleaned in isopropyl alcohol, immersed in methanol, and blow dried with dry nitrogen. It is concluded from separate experiments with a Tolansky interferometer that the Nichrome material is completely evaporated from the tungsten coil.

III. ARGON ION LASER EXPERIMENTS

Experiments were performed with a dc-excited discharge tube with an active plasma length of 60 cm and a 3-mm diameter bore. A Brewster-angle prism was used inside the cavity to select the desired laser transition; the cavity consisted of a 5-m mirror and a flat mirror separated by 150 cm. The metal film was situated 2 cm from the flat mirror. With this configuration, no adjustable aperture was required to obtain fundamental transverse mode operation.

Films of pure nickel or Nichrome were deposited on one side of a fused quartz plate. These plates were of optical quality suitable for

their use as Brewster-angle windows for laser tubes. In order to eliminate the effects of Fabry-Perot interferences between the front and back surfaces of the plates, an additional plate with an antireflection coating on one side was contacted with optical matching oil to the bare surface of the metal-coated plate.

The measurements reported here were made using this composite plate with an antireflection coating on one side and the metal film on the other. Virtually the same laser output power was observed when the simple plate with a metal film on one side, and no coating on the other, was used in the laser cavity.

Several films of different thickness of nickel and Nichrome were used for these experiments. The best results were obtained with a 150-Å Nichrome film. Because details of the deposition technique may affect the properties of the film obtained it is perhaps more informative to list the characteristics of the film measured with an external (traveling-wave) beam. These were

$$T = 0.60 \pm 0.01, \qquad R = 0.13 \pm 0.005, \qquad A = 0.27 \pm 0.01$$

for the beam incident on the metal film and

$$T = 0.61 \pm 0.01, \qquad R = 0.013 \pm 0.002, \qquad A = 0.38 \pm 0.01$$

for the beam incident on the antireflection coating. These measurements were made at 5145 Å. Virtually the same results were obtained at 4880 Å. These results were used to find the complex index of refraction used for the calculations in Section II. Figure 4a shows the laser output at 4880 Å as a function of the distance between the metal film and the end mirror of the laser cavity. This distance was varied by a ramp voltage applied to a piezoelectric ceramic transducer element on which the laser mirror was mounted. As the relative film position is varied, different longitudinal modes of the laser find themselves with a standing-wave minimum at the metal film and thus are able to oscillate. The overall outline of the pattern indicates the profile of the gain curve. The side humps are caused by the axial magnetic field applied to the laser tube.

In order to verify that we had indeed achieved single-frequency operation, a scanning interferometer was set up to observe the frequency spectrum of the laser output. Figure 4b shows the output versus frequency for the laser operating without a metal film in the cavity. This picture corresponds to the maximum available output of 500 mW at 4880 Å. With a 150-Å Nichrome film in the laser cavity,

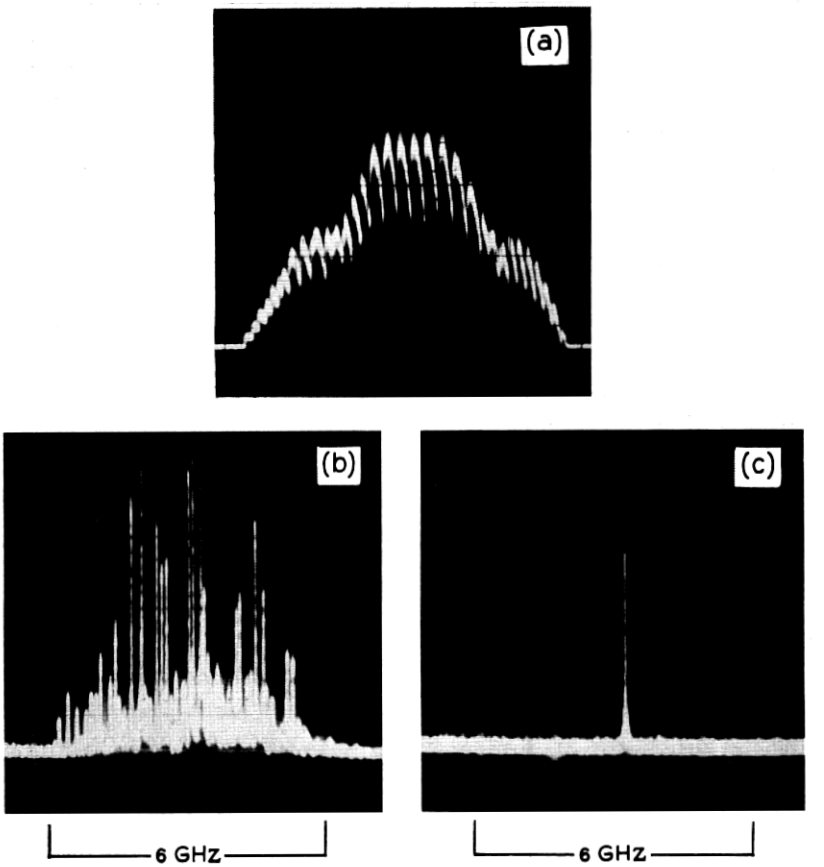

Fig. 4 — Experimental results using metal-film mode selector in an argon ion laser oscillating at 4880Å: (a) Single-frequency laser output as a function of separation between metal film and laser end reflector; (b) Multimode output of laser without mode selector as a function of frequency: total output power 500 mW. The total oscillation bandwidths is ≈6 GHz; (c) Single mode laser output obtained using metal film as a function of frequency: output power 350 mW.

single-frequency output was obtained at 4880 Å as shown in Fig. 4c. Over 350 mW or 70 percent of the multimode output could be obtained in a single frequency. At 5145 Å, 50 percent of the multimode power could be obtained in a single frequency, using the same film.

These figures can be compared with those for an interferometric mode selector of the type described in Ref. 4. A mode selector of that type was constructed for use with the argon ion laser. It was found

that with the same type of laser 50 percent of the multimode output power at 5145 Å could be obtained in single-frequency output; 70 percent of the multimode output power at 4880 Å could be obtained in single-frequency output. Thus, for this laser, the two schemes appear identical in power output.

From curve 2 of Fig. 2 we find that the loss produced by the metal film is less than the laser gain ($\approx$ 25 percent) for a frequency range of roughly 1.3 GHz. The fact that single-frequency operation was obtained with this film indicates that mode-competition effects must have extended over this range of frequencies. This is not surprising as the natural linewidth for the argon laser is about 500 MHz and radiation broadening will increase this homogeneous linewidth in a laser well above threshold.[5] Mode competition effects are expected between adjacent modes spaced by less than the homogeneous linewidth. Thus we see that, for the argon laser, single-frequency operation can be obtained with a much lower selectivity mode selector than would be required if mode competition were not present.

IV. *Nd:YAG* LASER EXPERIMENTS

4.1 *Description of the Laser*

The laser system consisted of a 30- by 2.5-mm neodymium: yttrium aluminum garnet (Nd:YAG) rod, pumped with a 1-kW tungsten lamp in an elliptic cylinder, a high reflectivity plane mirror, and an output mirror with 10-m curvature and 1.6 percent transmission. The mirror separation was $M = 20$ cm which resulted in a longitudinal mode spacing of 670 MHz. Without insertion of any mode selector, this cavity configuration gave fundamental transverse mode operation up to 850-W pump power. Figure 5a shows the output spectrum at that pump level observed with a scanning Fabry-Perot interferometer. The total output power was 200 mW with a maximum linearly polarized component of 130 mW. This component increased to 220 mW at 960-W pump power, but this power was not all in the fundamental mode, and the amplitudes of individual modes were very unstable.

To obtain single-frequency operation, the plane mirror was replaced by a fused silica flat 2.5 mm thick (free spectral range 40 GHz) which was high-reflectivity coated on one side and metal coated on the other. This arrangement produced stable single-frequency output, as evidenced by Fig. 5b, which was photographed from a screen averaging over 10 scans in one second (the persistance time of the screen). The output stability was achieved by keeping one particular node of one

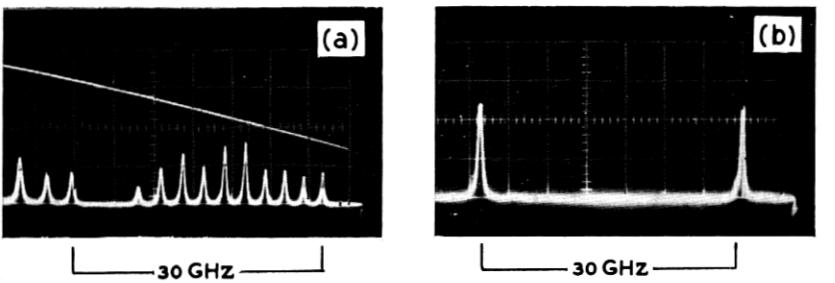

Fig. 5 — Experimental results using metal-film mode selector in neodymium-doped YAG laser oscillating at 1.06μ. (a) Multimode output of laser without mode selector as a function of frequency. Linearly polarized output power 130 mW. The frequency spacing between modes corresponds approximately to $c/2L$ for the YAG rod. The upper trace shows the ramp voltage used to scan the Fabry-Perot interferometer. The output spectrum display repeats itself with the spacing of the interferometer free spectral range (30 GHz). The total oscillation bandwidth of the laser shown here is $\approx$22 GHz. (b) Single mode laser output obtained using metal film as a function of frequency: linearly polarized output power 60 mW.

longitudinal mode close to the film center. Their relative positions should be within about ± 20 A since the nodes corresponding to adjacent longitudinal modes are spaced at $N_0 L\lambda/2M = 84$ Å in the vicinity of the film. This implies temperature stabilization of the quartz flat to within ± 0.1°C $[\partial(N_0 L)/L\partial T = 8 \times 10^{-6}/°\text{C}]$, and cavity length stabilization to within $\pm$1,000 Å. In addition, the film becomes inefficient if its tilt exceeds one adjacent longitudinal node spacing across the beam diameter. Thus the quartz flat must be parallel to about 2 seconds of arc and its flatness should be better than $\lambda/20$.

4.2 *Results*

Best results at lowest threshold were obtained with a 50-Å nickel-chromium film. Its transmission and reflection, as measured with a YAG laser beam, are shown in Table I. A power of 60 mW (maximum linearly polarized component) could be obtained in a single frequency which was 27 percent of the maximum multimode power output. However, the absorption of the film was not sufficient to obtain single-frequency output up to the pump limit. At 960 watts pump power, the total (multimode) output power was 150 mW with a frequency range of 4 GHz. Curve 1 of Fig. 2 predicts a 4 GHz range for a net gain of 3 percent ($c/N_0 L = 80$ GHz). In addition it was observed that the output was much more stable than that of the free-running laser: the power in an individual mode was constant to within 20 percent.

Therefore, inserting a metal film into the cavity is a simple technique for obtaining a stable YAG laser output in a narrow frequency range.

Several other films have been tried. A 100-Å nickel-chromium film, for instance, had close to zero minimum reflectance according to curve 3 of Fig. 2. This curve was calculated from the transmission (48 percent) and reflections (18 percent and 32 percent) measured with a YAG laser beam. It was verified that the minimum loss was larger than for the 50-Å film since the threshold for oscillation had increased to 800 W pump power (compared with 600 W for the 50-Å film). Although curve 3 in Fig 2 indicates a higher selectivity for this film, the maximum single-frequency output was again 60 mW. If the pump power was increased beyond this point, multimode operation was obtained.

Obviously, the metal film technique works less efficiently for the YAG laser than for the argon ion laser. The reasons for this are (*i*) the apparent lack of mode competition which makes it necessary for the YAG laser to completely suppress all but one mode (not just to provide a little more loss for the other modes), and (*ii*) its low gain which makes the YAG laser output very sensitive to small additional losses. Therefore, it is generally much more difficult to obtain a high-power single-frequency output from a YAG laser than from an argon ion laser or helium-neon laser.

V. DISCUSSION AND CONCLUSION

The theoretical and experimental results show that it is possible, under suitable circumstances, to obtain high-power single-frequency operation of a laser using the metal film technique. In practice, however, it is not always possible to find a material that has the required loss in a sufficiently thin film. This is in contrast with interferometric mode selectors whose selectivities are determined simply by the reflectivities of the elements. For the argon ion laser an interferometric mode selector has some advantages over the metal film;[4] however, it is difficult to apply to the YAG laser because of its much greater oscillation width (about 100 GHz). The metal film method described here does have the advantage of simplicity, however, and the system is relatively easy to make mechanically stable. The metal film technique should be of particular interest to people working in the fields of Brillouin scattering or holography where a narrow bandwidth source is required. It is relatively easy with a metal film to restrict the laser oscillation to a few neighboring modes. Thus a drastic re-

duction in bandwidth can be made, often at little expense in total output power.

VI. ACKNOWLEDGMENTS

We wish to thank Mr. P. J. Maloney and Mr. J. M. Barro for technical assistance, Mr. S. Shah for evaporating the metal films, and Mr. D. W. Doughty for making the dielectric coatings.

REFERENCES

1. Troitskii, Yu. V. and Goldina, N. D., "Separation of One Mode of a Laser," J. Experimental and Theoretical Phys. Letters, *7,* (January 30, 1968) pp. 36–38.
2. Troitskii, Yu V. and Goldina, N. D., "Thin Scattering Film in the Field of a Standing Wave of Optical Frequencies and its Use in Selecting Modes of an Optical Resonator," Opt. Spectroscopy, *25,* No. 3 (September 1968), pp. 255–256.
3. Wolter, H., "Optik Dünner Schichten," *Handbuch der Physik,* Springer-Verlag, Berlin, 1956, *24,* pp. 461–473.
4. Smith, P. W., "Stabilized, Single-Frequency Output From a Long Laser Cavity," IEEE J. Quantum Elec., *QE1,* No. 11 (November 1965) pp. 343–348; and "On the Stabilization of a High-Power Single-Frequency Laser," IEEE J. Quantum Elec., *QE2,* No. 9 (September 1966) pp. 666–668.
5. Webb, C. E., Miller, R. C., and Tang, C. L., "New Radiative Lifetime Values for the 4s Levels of AII," IEEE J. Quantum Elec. *QE4,* (May 1968), p. 357.